


Effect of microridges on the performance of three-lobe journal bearing considering cavitation and lubricant compressibility

Basim A. ABASS ^{1,*}, Mushrek A. MAHDI ²

¹ College of Engineering, University of Babylon, Hillah, Iraq

² Al-Musayyab College of Engineering, University of Babylon, Hillah, Iraq

*Corresponding author: eng.basim.ajeel@uobabylon.edu.iq

Keywords

three-lobe bearing
micro ridges
cavitation effect
compressibility effect
hydrodynamic lubrication

Abstract

This study presents a numerical study of the effect of microridges on the performance of the three-lobe journal bearing considering lubricant compressibility and cavitation effects. A mathematical model based on the Reynolds equation that has been modified to take into account the effects of lubricant compressibility and cavitation has been proposed to achieve the primary goal of this work. Lubricant compressibility is considered by using lubricating oils with different bulk moduli while Elord's algorithm was used to consider the effect of cavitation. The governing equations for finite length journal bearing lubricated with Newtonian oil in laminar flow and isothermal condition are numerically discretised using the finite difference method and solved by using a suitable prepared computer program. The performance of the rough and smooth bearings was compared for plain and three-lobe journal bearings. The numerical model was demonstrated by comparing the pressure distribution for smooth and microridges three-lobe journal bearing with that published by El-Said et al. and they were found in good agreement. It was found that the pressure and the load were considerably enhanced and the coefficient of friction decreased by 15 % for three-lobe journal bearing with microridges in comparison with that of smooth surfaces.

History

Received: 31-08-2023

Revised: 03-10-2023

Accepted: 06-10-2023

1. Introduction

Three-lobe journal bearing is a noncircular journal bearing widely used in high-speed lightly loaded rotating machinery due to its better dynamic characteristics compared with cylindrical journal bearings, which suffer from instabilities in these circumstances. The analysis of three-lobe journal bearing was extensively considered by different authors [1-3]. Among the previous works, Etsion [4] shows that surface irregularity has a considerable effect on improving the surface attainment of journal bearings over a wide range of operating modes. The microdents formed on the surface can act as micro-hydrodynamic bearings in full or mixed lubrication with either incompressible or compressible lubricants. Bayada et al. [5]

studied the effect of micro- and macro-roughness on the elastohydrodynamic performance of journal bearing using the Jacobson-Floberg-Olson (JFO) mass flow model to preserve the cavitation and the elastohydrodynamic effects. The efficiency of journal bearing surface texturing was determined by a fluid flow model in a single micro-scale irregularity unit cell implemented by de Kraker et al. [6] using Navier-Stokes equations rather than Reynolds equation. Dhande et al. CFD-FSI technique presented in [7] was used by Meng et al. [8] to investigate the influence of a complex dimple on the tribological behaviour of the journal bearing. It was found that depending on the geometry and size of the compound dimples, as well as the bearing's operating parameters, a higher load might be followed by a lower coefficient of friction.

The effect of different surface texture patterns and different depths on the performance of the



This work is licensed under a Creative Commons Attribution-NonCommercial 4.0 International (CC BY-NC 4.0) license

bearing with parallel sliding surfaces was extensively studied [9-12]. It was observed that the depiction of such bearings was influenced by the form and the kind of texture. The surface texture may be the only cause of the hydrodynamic lubrication of the parallel surfaces moving on each other as stated by Noutary et al. [13]. The numerical analysis shows that only partial texturing must be used to generate positive load capacity. In another work, inlet textured journal bearing with different texture lengths lubricated with a temperature-dependent fluid was analysed numerically by Cupillard et al. [14]. The surface texture shows a stronger and more positive influence on load capacity when thermal effects are considered. The effect of an optimised elliptical cavity with diverse depths, diameters, area ratios and different operating conditions on the coefficient of friction of hydrodynamic journal bearing was studied by Ma and Zhu [15]. Codrignani et al. [16] show that the dimple depth has a higher significance than the diameter in determining the optimal texture shape. The effect of longitudinal, isotropic and transverse roughness on the pressure distribution over rough surfaces of multi-lobe journal bearing was studied by PhaniRaja Kumar et al. [17]. It was found that longitudinal surface roughness has more effect than transverse and isotropic roughness on the performance of such bearing. The static and dynamic performance of partial slip texture multi-lobe journal bearings was studied by Rao et al. [18]. It was found that this configuration significantly enhances the load, the coefficient of friction and the stability of the two-lobe journal bearing.

A great reduction in the bearing coefficient of friction with a shift in the transition from mixed to hydrodynamic lubrication, at low rotational speeds was observed due to the single- and multi-scale surface patterns as stated by Grützmaier et al. [19] and König et al. [20]. El-Said et al. [21] deal with the effect of uniform micro protrusions on the steady-state and dynamic performance of three-lobe journal bearing. The load-carrying capacity and the coefficient of friction were enhanced due to the existence of such protrusions. The combined effect of surface roughness and couple stress fluid on the elastohydrodynamic performance of journal bearing was studied by Chiang et al. [22] and Nabhani et al. [23]. It was observed that the interaction between couple stress, surface roughness and elastic deformation effects is significant. Rom and Müller [24] show that the flow of lubricant with high velocities and surfaces with

deep texture and moderate length requires the solution of Navier-Stokes equations rather than the Reynolds equation. The effect of isotropic surface texture on the thermal turbulent lubrication of misaligned journal bearing was studied by Zhu et al. [25]. It was found that the maximum film pressure, load capacity and misalignment moment of the bearing increase with the increase of the surface roughness height and the degree of misalignment.

The effect of surface roughness on the thermal behaviour of the journal bearing was studied by Tala-Ighil and Fillon [26]. More realistic results for the performance parameters were obtained. The CFD approach was used by Sahlin [27] to explore the domination of using miscellaneous artificial microscopic surface designs of the two interacting surfaces on the frictional interpretation of journal bearing. The combined effect of wear and surface roughness on the performance of misaligned journal bearing considering cavitation was studied by Jang and Khonsari [28] using a suitable computational model. The obtained results show that the wear was affected by surface irregularity, contact pressure and film thickness. Gu et al. [29] used the mass conservation approach to reformulate the Elrod-Adams cavitation model to study the combined effect of cavitation and random surface roughness on the performance of journal bearings. Venci et al. [30] stated that surface texturing is one of the surface modification techniques used to improve, among other things, its tribological performance. Guidance for the optimal design of surface textures in practical engineering applications has been provided. Different studies related to the tribological properties of ZA27/SiC/Gr hybrid composite materials that can be used as a bearing material have been performed experimentally [31] and analytically [32].

It is clearly shown from the presented studies that the combined effect of different parameters on the performance of rough surface journal bearings seems to be important for more realistic results. The main goal of this study is to study the steady-state performance of microridges three-lobe journal bearing considering the lubricant compressibility and cavitation effects which are rarely studied.

2. Mathematical model

A finite length three-lobe journal bearing shown in Figure 1, with geometrical and operating parameters shown in Table 1, was mathematically modelled using the finite difference technique to

study the combined effects of microridges, lubricant compressibility and cavitation on the performance of such bearing. The bearing consists of three lobes, and the centre of each lobe is displaced an equal distance from the centre of the bearing. The maximum span of each lobe is 120° .

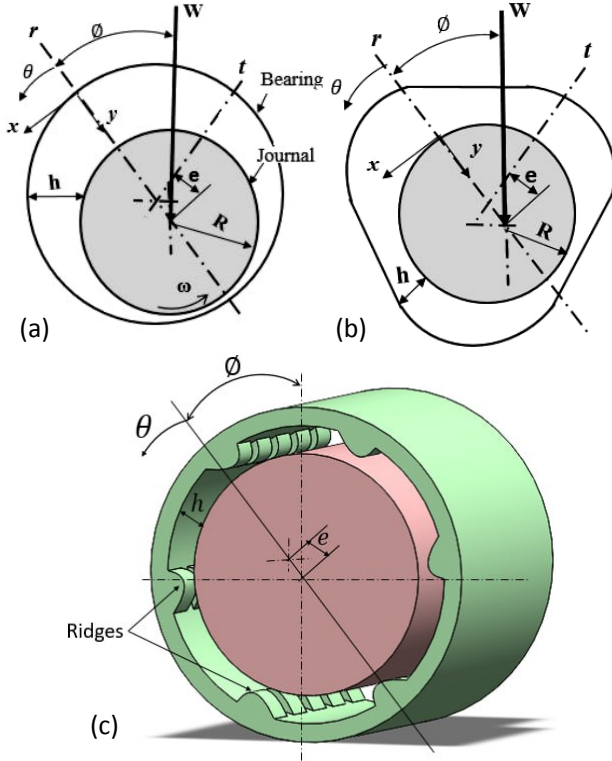


Figure 1. Geometry of cylindrical and three-lobe journal bearings: (a) plain journal bearing, (b) three-lobe journal bearing and (c) expected distribution of the ridges on the bearing surface

Table 1. Geometrical properties of the journal bearing

Property	Value
Bearing length L	60 mm
Journal diameter D	60 mm
Radial clearance c	145 μm
Rotational speed N	2000 rpm
Atmospheric pressure P_a	101.325 Pa
Inlet lubricant viscosity μ_o	0.0277 Pas
Cavitation zone pressure P_{cav}	0.0 Pa
Lubricant bulk modulus β	6.7×10^9 Pa
Dimensionless bulk modulus $\bar{\beta}$	30, 40, and 50
Ridges height H_a	0.1, 0.3 and 0.5 μm
Ridges width in x and z direction $n_x = n_z$	6 μm
Number of lobes n_w	3
Geometry factor m	1.0
Wave amplitude ε_w	0.1 – 0.25 μm

With the assumptions stated that the flow of lubricant was laminar and lubricant was Newtonian and isothermal, the following Reynolds equation is utilised to estimate the distribution of lubricating oil pressure [33]

$$\frac{\partial}{\partial x} \left(\frac{\rho h^3}{\mu} \frac{\partial P}{\partial x} \right) + \frac{\partial}{\partial z} \left(\frac{\rho h^3}{\mu} \frac{\partial P}{\partial z} \right) = 6U \frac{\partial \rho h}{\partial x}, \quad (1)$$

where U is the tangential velocity in m/s.

In the cavitation zone, the pressure remains constant (i.e. $P = P_{\text{cav}}$). The mass conservation in the oil film rupture and reformation location was concerned with the mass conserving boundary condition. The pressure gradient was assumed to be zero in the cavitation zone. The cavitation algorithm contains a switch function to modify the Reynolds equation in this zone. The oil film pressure, density, and switch function g are related through the lubricant bulk modulus β using the following equation [33]

$$\beta = \rho \frac{\partial P}{\partial \rho} = \varphi \frac{\partial P}{\partial \varphi}. \quad (2)$$

Equation (2) can be integrated to give [33]

$$P = P_{\text{cav}} + g\beta \ln(\varphi), \quad (3)$$

where P_{cav} is the lubricant pressure in the cavitation zone and φ is the density ratio variable (fractional film content) given as [33]

$$\varphi = \frac{\rho}{\rho_{\text{cav}}}, \quad (4)$$

where ρ_{cav} is the lubricant density in the cavitation zone.

The switch function g is defined as

$$g = 0 \quad \text{in the inactive zone} \quad \varphi < 1$$

$$g = 1 \quad \text{in the active zone} \quad \varphi \geq 1$$

Introducing Equations (2), (3) and (4) into Equation (1) and using the following dimensionless form

$$x = R\theta, \quad z = \bar{z}L, \quad \beta = \frac{\mu_o U R \bar{\beta}}{c^2}, \quad \mu = \mu_o \bar{\mu}, \quad \bar{h} = \frac{h}{c} = 1 + \varepsilon \cos \theta$$

the Reynolds equation in the dimensionless formula can be written as

$$\frac{\partial}{\partial \theta} \left(g \bar{\beta} \bar{h}^3 \frac{\partial \varphi}{\partial \theta} \right) + \left(\frac{R}{L} \right)^2 \frac{\partial}{\partial \bar{z}} \left(g \bar{\beta} \bar{h}^3 \frac{\partial \varphi}{\partial \bar{z}} \right) = 6 \frac{\partial}{\partial \theta} (\varphi \bar{h}). \quad (5)$$

The oil film pressure distributions are found from the fractional film content φ as

$$\bar{P} = \begin{cases} \bar{P}_{\text{cav}} + \bar{\theta} \ln(\varphi) & \text{if } \varphi \geq 1 \\ \bar{P}_{\text{cav}} & \text{if } \varphi < 1 \end{cases} \quad (6)$$

The oil film pressure is $\bar{P} = 0$ at $\bar{z} = 0$ and $\bar{z} = 1$. For journal bearing with microridges, the lubricant film thickness can be expressed as [21]

$$\bar{h} = 1 + \varepsilon \cos \theta - \Delta^*(\theta, \bar{z}) + \varepsilon_w \cos n_w \theta, \quad (7)$$

where Δ^* is film thickness variation measured from the stationary bearing surface (dimensionless).

The lubricant film thickness for a bearing with smooth surfaces can be expressed as

$$\bar{h} = 1 + \varepsilon \cos \theta. \quad (8)$$

The following mathematical protrusion profile suggested by [21] was used to investigate the hydrodynamic lubrication effect of the dimensional bearing surface irregularities.

$$\Delta^* = \left(\frac{H_a}{c} \right) \sin^{2m} \left[\pi \left(\frac{\theta n_x}{2\pi} - 1 \right) \right] + \sin^{2m} \left[\pi (\bar{z} n_z - 1) \right], \quad (9)$$

where m is the geometry factor. A smaller value of m means that the roughness profile (ridge) takes on a concave shape in both the axial and circumferential directions, as it is shown together with n_x , n_z and H_a in Figure 2.

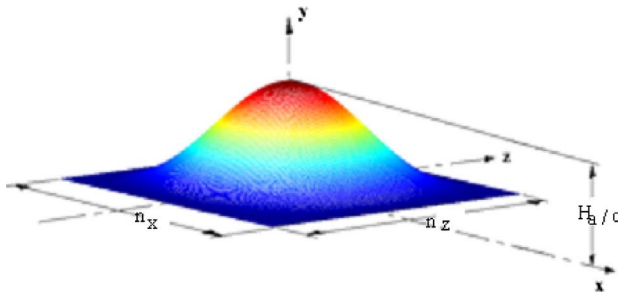


Figure 2. Roughness profile; reprinted from [El-Said et al. \[21\]](#), licensed under [CC BY-NC-ND 4.0](#)

3. Performance characteristics of bearing

The load-carrying capacity of the journal bearing is given as

$$W = \sqrt{W_r^2 + W_t^2}, \quad (10)$$

where

$$W_r = \frac{\bar{W}_r \mu L U R^2}{c^2} \int_0^{2\pi} \int_0^1 \bar{P} \cos \theta d\theta d\bar{z}, \quad (11)$$

$$W_t = \frac{\bar{W}_t \mu L U R^2}{c^2} \int_0^{2\pi} \int_0^1 \bar{P} \sin \theta d\theta d\bar{z}. \quad (12)$$

The attitude angle ϕ can be calculated from the following equation

$$\phi = \tan^{-1} \left(-\frac{W_t}{W_r} \right). \quad (13)$$

The friction force of the journal can be expressed as

$$F_r = \frac{\mu L U R}{c} \int_0^{2\pi} \int_0^1 \left(\frac{1}{\bar{h}} + \frac{\bar{h}}{2} \frac{\partial \bar{P}}{\partial \theta} \right) d\theta d\bar{z}, \quad (14)$$

and the coefficient of friction is given as

$$C_f \left(\frac{R}{c} \right) = \frac{F_r}{W}. \quad (15)$$

The Sommerfeld number S_o can be found from the relation

$$S_o = \frac{\mu N}{P} \left(\frac{R}{c} \right)^2. \quad (16)$$

4. Computational algorithm

The performance study of a three-lobe journal bearing considering the effect of microridges, lubricant compressibility and cavitation effects required the numerical solution of Equation (5) with appropriate boundary conditions. The finite-difference technique was adopted to solve the Reynolds equation using a direct iterative procedure with successive underrelaxation (SUR) method to find the φ distribution. The computational process involves the following steps:

- The film domain is divided into 120 intervals along the circumferential direction and 20 intervals in the axial direction.
- Input of the operating conditions and lubricant properties.
- Calculation of the initial value of φ is restricted as a first step in the solution process, which can be predicted as

$$\phi = \tan^{-1} \left[\frac{\pi}{4\varepsilon} (1 - \varepsilon^2)^{1/2} \right]. \quad (17)$$

- Assumption of an initial value of φ and g in the active region for the first iteration.
- Obtaining the film thickness at each node from Equation (7).

- Computing of the new distributions of φ by an iterative solution of Equation (5), using a suitable under-relaxation factor. The switch function at all points is updated after each iteration, based on the new values of φ . The total loop of the iteration is stopped when the convergence criterion of the variable φ reaches 10^{-5} .
- Calculation of the film pressure from Equation (6) and updating of the film geometry.
- Computing the components of the load capacity from Equations (11) and (12) after which a new value of attitude angle ϕ can be obtained from Equation (13) and compared with an old value of the angle. The iteration is stopped when the convergence criterion of ϕ reaches 10^{-4} .
- Calculating the performance characteristics of the bearing.

The general procedure for the numerical computation is described in the flowchart as shown in Figure 3.

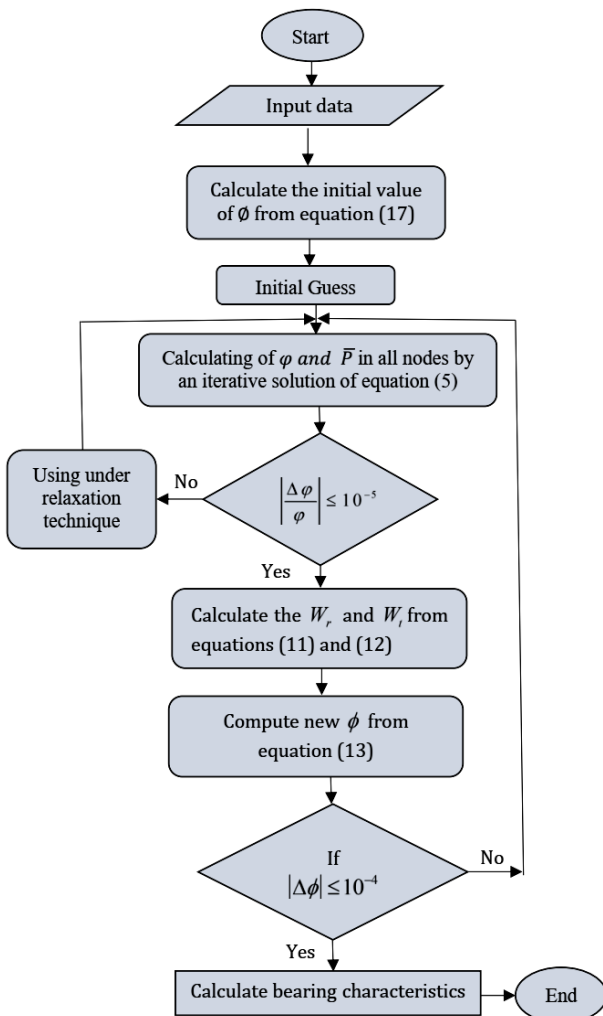


Figure 3. Flowchart of the general computational procedure

5. Results and discussion

The performance of journal bearing with microridges including cavitation and lubricant compressibility effects was extensively studied in this work. The mathematical model of this study was verified in our previous paper [34] by correlating the pressure distribution of smooth and microridges journal bearing with that achieved by El-Said et al. [21], as can be shown in Figure 4.

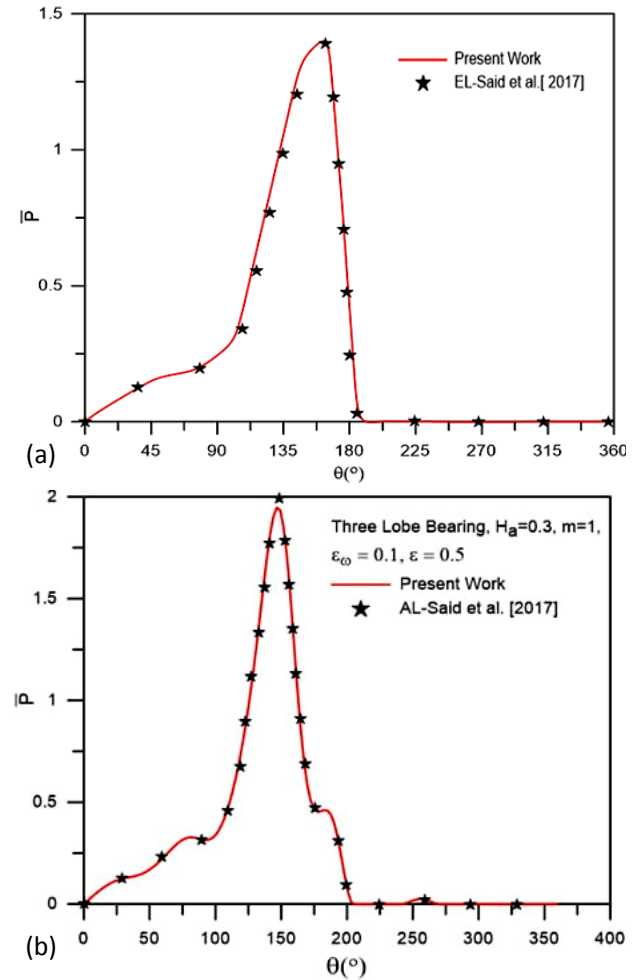


Figure 4. Pressure distribution: (a) smooth surfaces reprinted from Mahdi and Abass [34] licensed under CC BY-NC-ND 4.0 and (b) rough surface

This figure shows a good agreement between the results obtained in this study and those published in [21]. The variation of circumferential pressure for both plain and three-lobe journal bearings with smooth and microridges can be shown in Figure 5. The effect of using microridges with different heights ($H_a = 0.1, 0.3$ and $0.5 \mu\text{m}$) has been studied.

This figure shows that the oil film pressure generated in a three-lobe journal bearing is higher than that generated in a plain journal

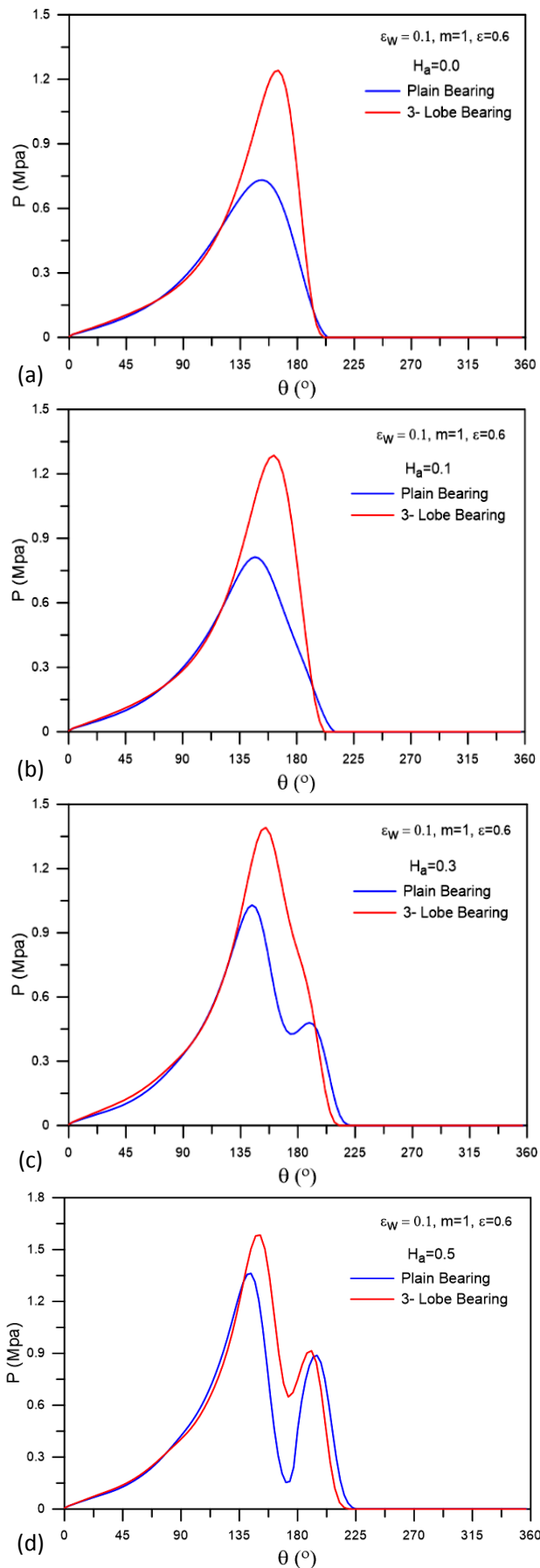


Figure 5. Circumferential pressure distribution for plain and three-lobe journal bearing: (a) $H_a = 0 \mu\text{m}$, (b) $H_a = 0.1 \mu\text{m}$, (c) $H_a = 0.3 \mu\text{m}$ and (d) $H_a = 0.5 \mu\text{m}$

bearing. It can be also observed that the oil film pressure becomes higher for the bearings with microridges that have higher amplitude. The pressure varies from 1.2 MPa for a bearing with a smooth surface to 1.6 MPa for a bearing with a rough surface with $H_a = 0.5 \mu\text{m}$. It can also be shown from this figure that the pressure rapidly dropped locally and then increased at the cavitation zone of the bearing due to the existence of the microdimples. This was supported by reference [35]. The pressure drop increases as the surface with protrusions of larger heights and this phenomenon is more severe in plain journal bearing than that in three-lobe journal bearing.

The point of maximum pressure for the three-lobe bearing moves toward the inlet of the bearing with different values depending on the height of the ridges. It has been noticed that the point of maximum pressure is at 171° for three-lobe with smooth surfaces ($H_a = 0 \mu\text{m}$) while it moves to 144° for rough three-lobe bearing with ridges height of $H_a = 0.5 \mu\text{m}$. Figure 6 shows that the inclusion of the cavitation effect causes a decrease in the bearing oil film pressure generated for both types of bearings. The position of the bearing maximum pressure for the three-lobe journal bearing was found to be 162° for the bearing with smooth surfaces and 139.5° for the rough three-lobe journal bearing with a ridges height of $H_a = 0.5 \mu\text{m}$.

Figure 7 shows that the existence of microroughness on the three-lobe bearing surface enhances the bearing load-carrying capacity. The higher the roughness height the higher the load carried by the bearing. The enhancement percentage in load-carrying capacity of the three-lobe journal bearing has been calculated and found to be 10 % for a bearing with ridges height of $H_a = 0.1 \mu\text{m}$, while it becomes 30 % for the bearing with ridges height of $H_a = 0.3 \mu\text{m}$. This figure also shows that the three-lobe journal bearing has a higher load-carrying capacity than plain journal bearing by 43.6, 56 and 42 % for ridges height of $H_a = 0$, 0.1 and 0.3 μm , respectively.

Figure 8 shows the Sommerfeld number of different bearings with smooth and microridges surfaces when they work at different eccentricity ratios. It can be observed from this figure that the Sommerfeld number decreases as the eccentricity ratio grows. Three-lobe journal bearing with ridges high of $H_a = 0.3 \mu\text{m}$ has the lowest values of the Sommerfeld number.

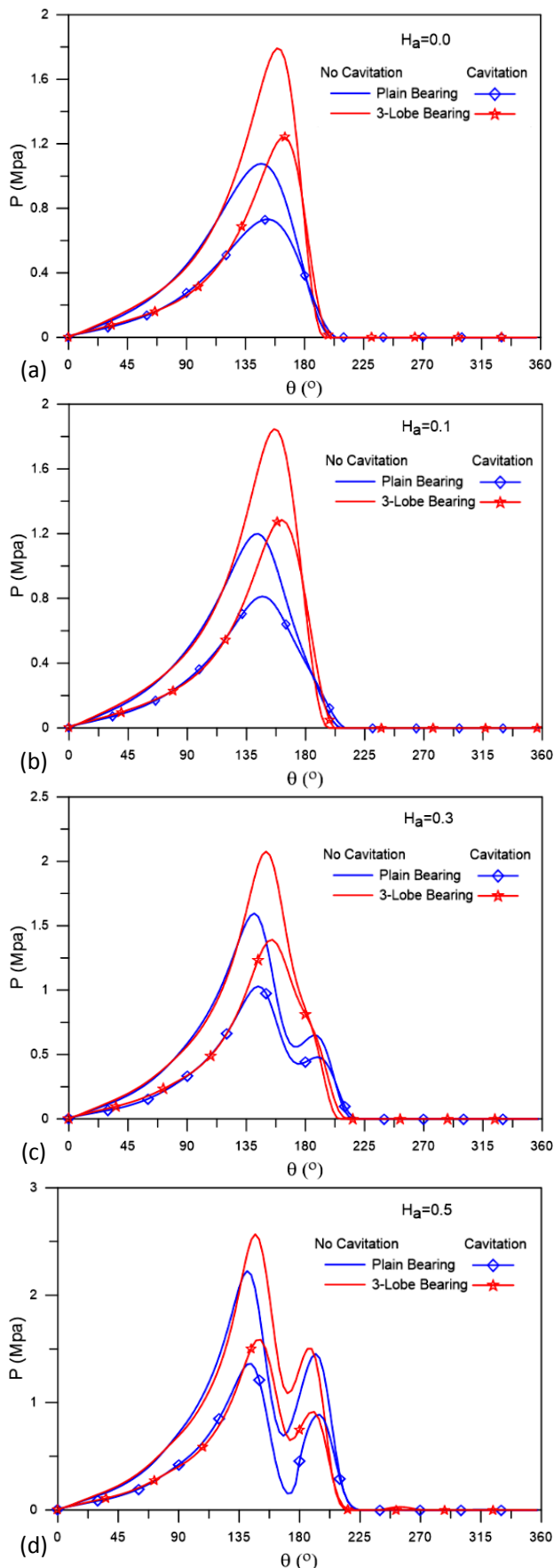


Figure 6. Effect of cavitation on circumferential pressure distribution for plain and three-lobe journal bearing: (a) $H_a = 0 \mu\text{m}$, (b) $H_a = 0.1 \mu\text{m}$, (c) $H_a = 0.3 \mu\text{m}$ and (d) $H_a = 0.5 \mu\text{m}$

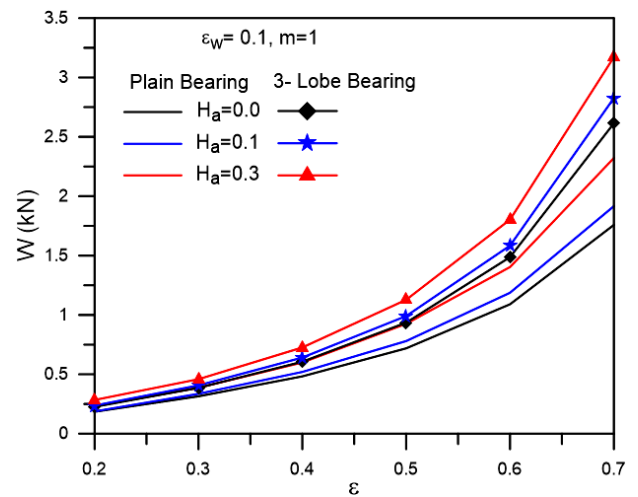


Figure 7. Effect of eccentricity ratio on load-carrying capacity for rough plain and three-lobe journal bearing

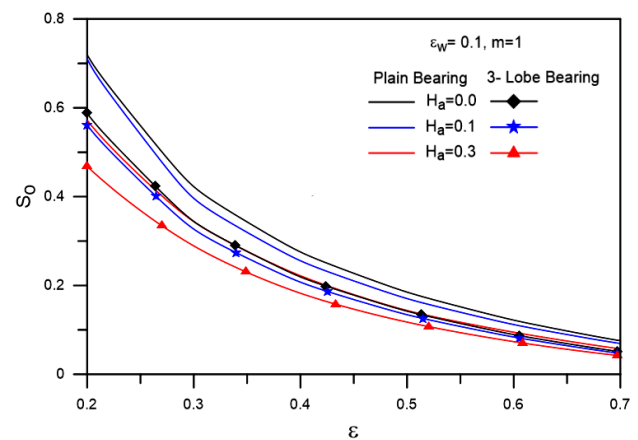


Figure 8. Sommerfeld number vs. eccentricity ratio for rough plain and three-lobe journal bearing

Figure 9 shows the variation of fractional film content distribution with the angular position of the bearings. It is well known that the fractional film content is greater than one at the full film region, while it is less than one at the cavitation zone [36]. It can be observed that the active region of the bearings increases for the bearings with a higher H_a . The end of the active zone for a three-lobe journal bearing is 202.5° , 211.5° , 216° and 220.5° for a bearing with $H_a = 0, 0.1, 0.3$ and $0.5 \mu\text{m}$, respectively.

The coefficient of friction for plain as well as three-lobe bearings has been calculated and presented in Figure 10. It can be seen from this figure that the bearing coefficient of friction decreases as the bearing works at a higher eccentricity ratio and has a higher roughness value. The percentage decrease of the coefficient of friction for a rough three-lobe journal bearing with ridges high of $0.3 \mu\text{m}$ is 15 % in comparison with that of a smooth surface. The roughness has little effect on the coefficient of friction when the

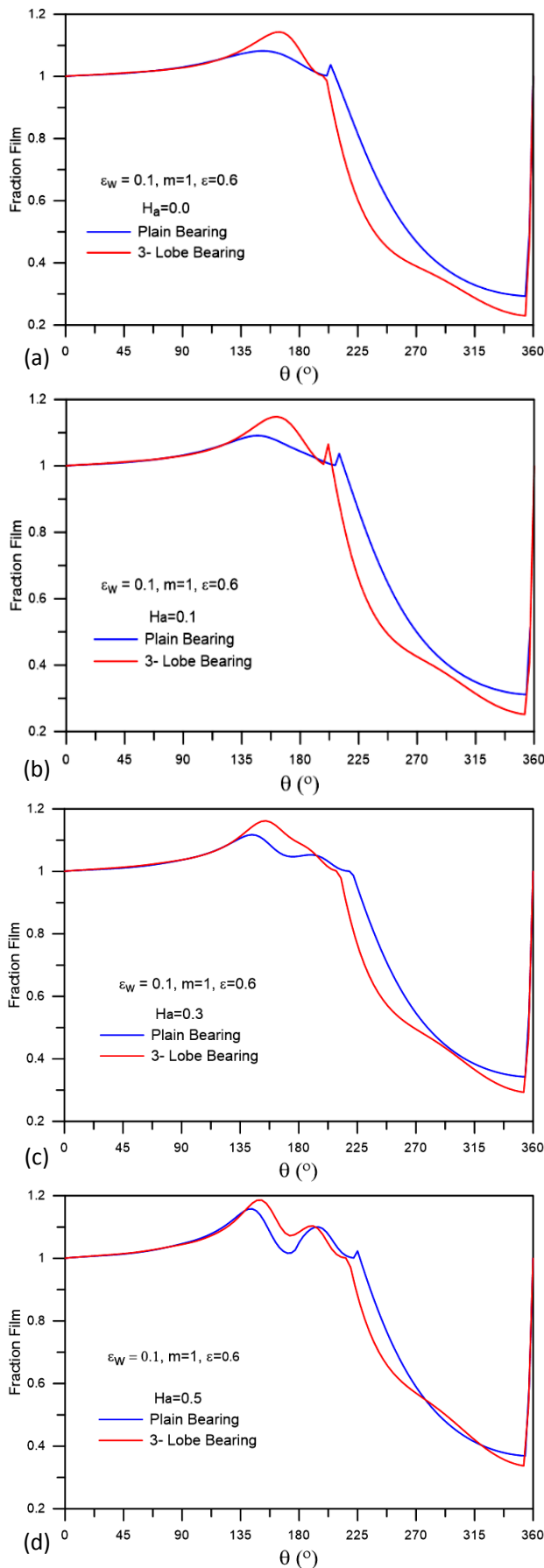


Figure 9. Fraction film content vs. angular position for smooth and rough journal bearing: (a) $H_a = 0 \mu\text{m}$, (b) $H_a = 0.1 \mu\text{m}$, (c) $H_a = 0.3 \mu\text{m}$ and (d) $H_a = 0.5 \mu\text{m}$

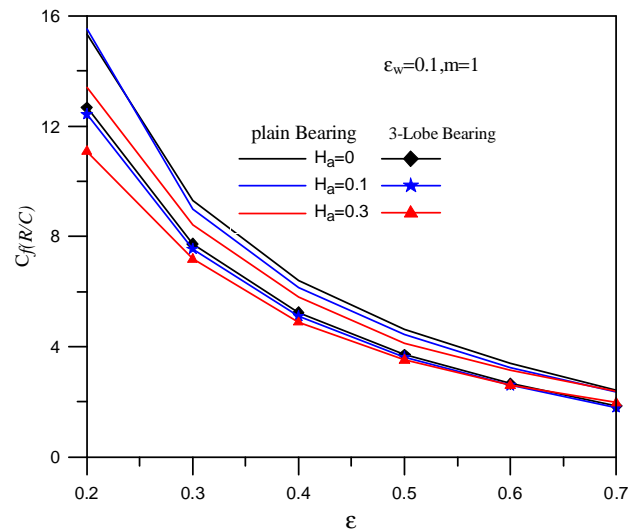


Figure 10. Coefficient of friction vs. eccentricity ratio for plain and three-lobe journal bearing

bearing is working at higher eccentricity ratios. This can be attributed to the higher load carried by the bearing in this case.

The effect of wave amplitude ε_w on the pressure distribution of rough three-lobe journal bearing can be seen in Figure 11. The wave amplitude seems to have little effect on the oil film pressure and it becomes negligible for the bearing with higher H_a . The maximum pressure occurs between 153 and 173°.

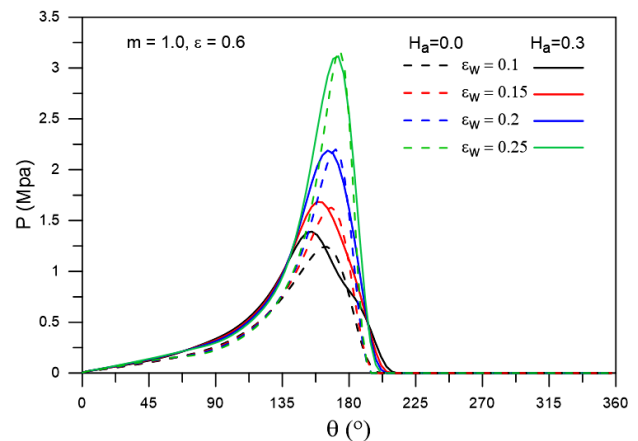


Figure 11. Effect of wave amplitude on the circumferential pressure distribution

Figure 12 shows the effect of wave amplitude ε_w on the fractional film content distribution. This figure shows that the range of the active zone becomes smaller for the bearing with a higher value of wave amplitude.

The effect of lubricant compressibility was studied by using lubricants with different dimensionless bulk modulus $\bar{\beta}$ as can be seen in Figure 13. It seems that the compressibility of lubricant has an insignificant effect on the generated oil film pressure.

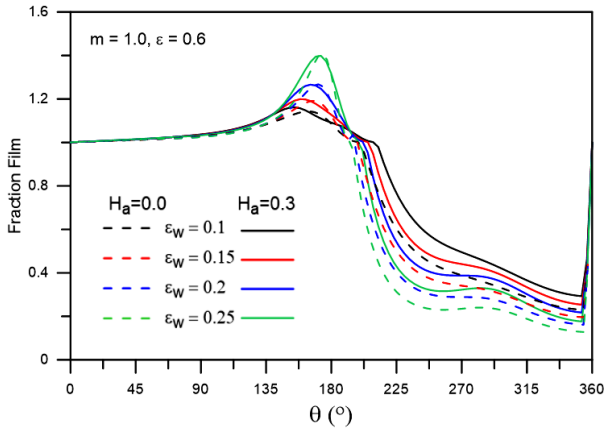


Figure 12. Effect of wave amplitude ε_w on the variation of fractional film content

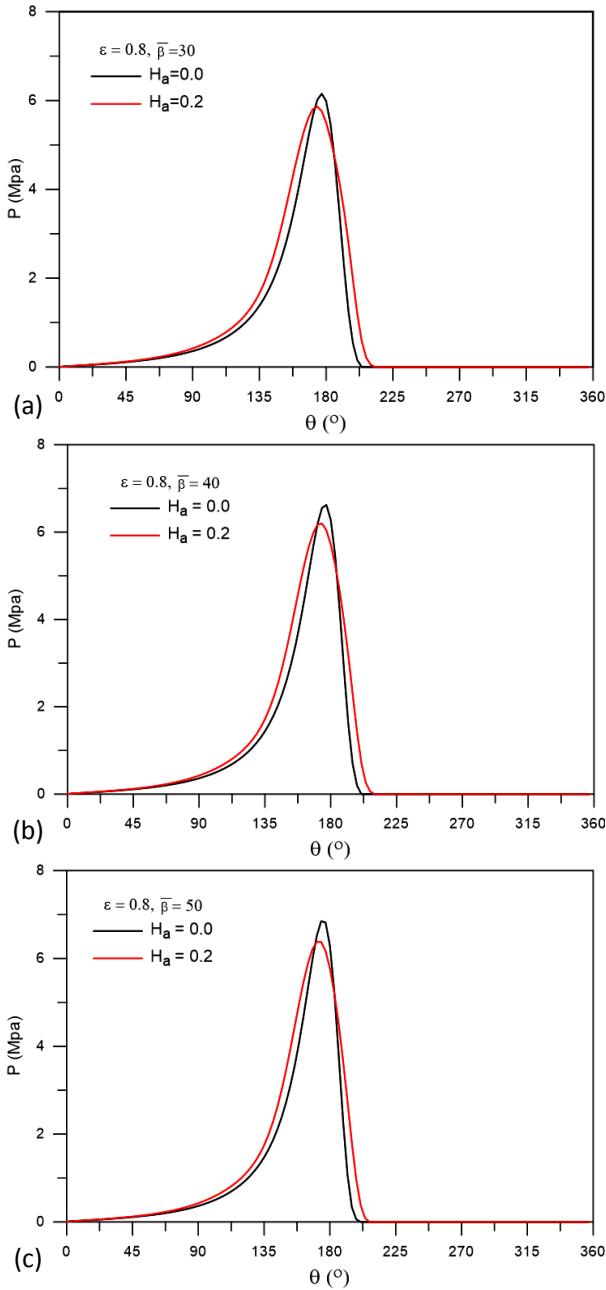


Figure 13. Effect of lubricant compressibility on the pressure distribution of three-lobe bearing with $\varepsilon_w = 0.8$: (a) $\bar{\beta} = 30$, (b) $\bar{\beta} = 40$ and (c) $\bar{\beta} = 50$

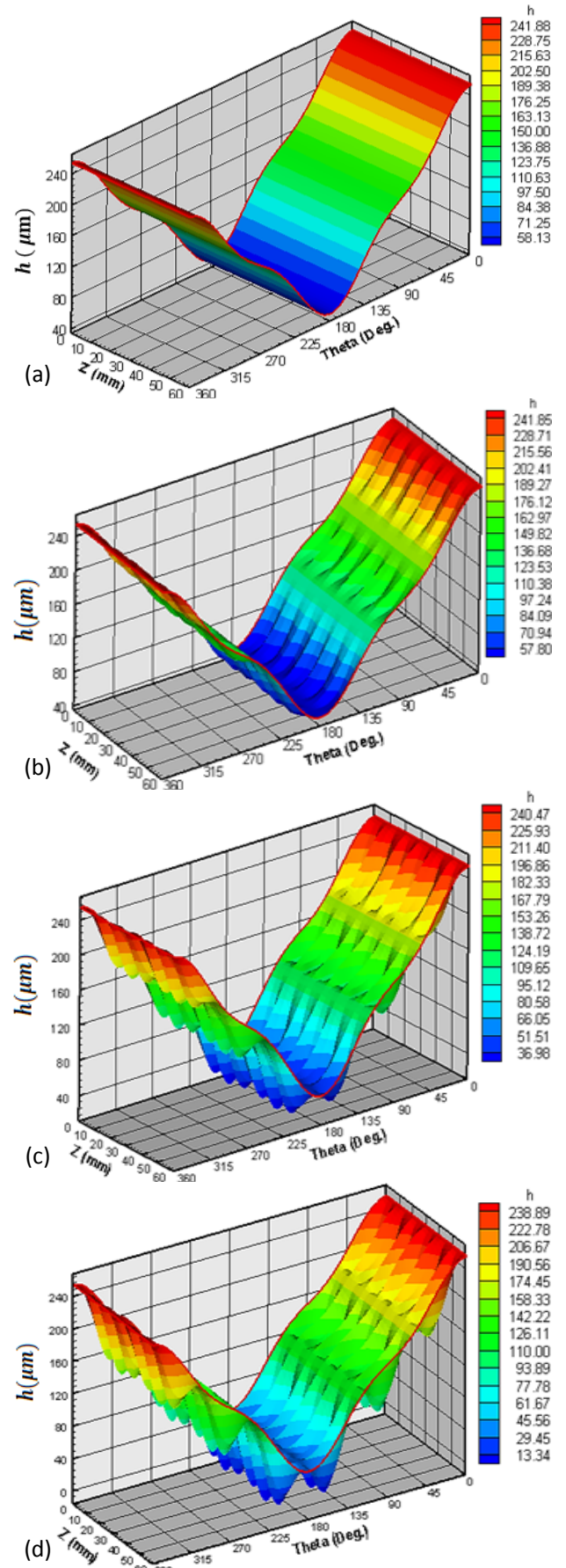


Figure 14. Effect of ridges height on the oil film thickness at $\varepsilon_w = 0.1 \mu\text{m}$, $\varepsilon = 0.6$ and $m = 1$: (a) $H_a = 0 \mu\text{m}$, (b) $H_a = 0.1 \mu\text{m}$, (c) $H_a = 0.3 \mu\text{m}$ and (d) $H_a = 0.5 \mu\text{m}$

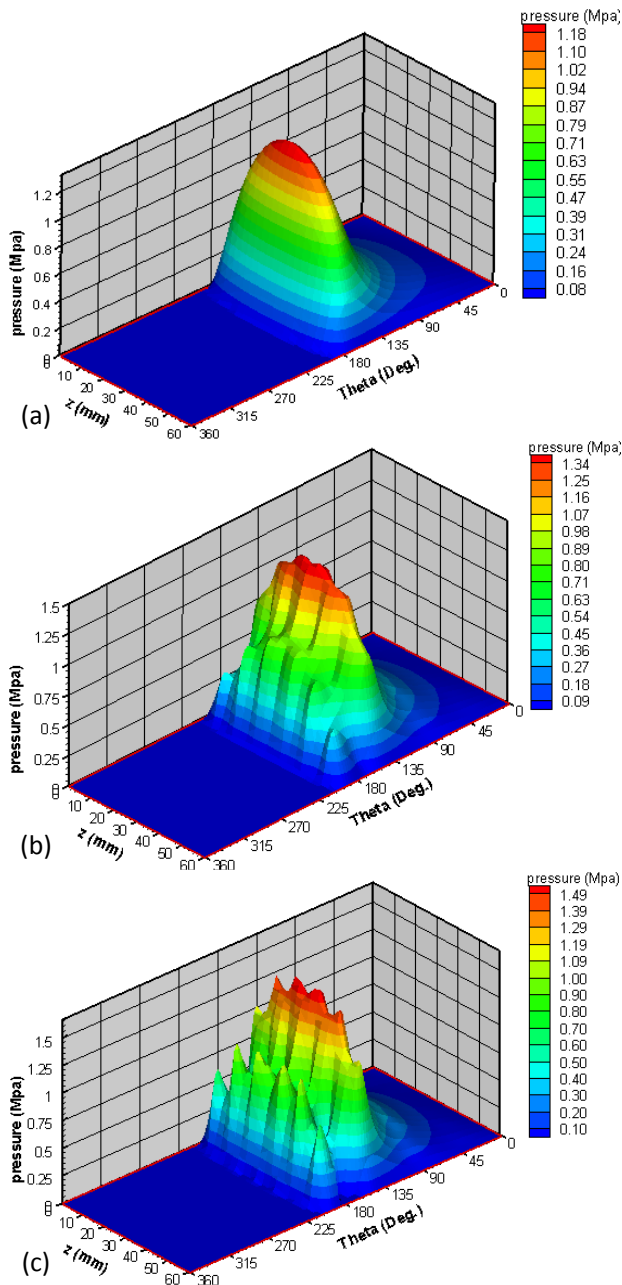


Figure 15. Oil film pressure variation in both axial and circumferential directions at $\epsilon_w = 0.1 \mu\text{m}$, $\epsilon = 0.6$ and $m = 1$: (a) $H_a = 0 \mu\text{m}$, (b) $H_a = 0.3 \mu\text{m}$ and (c) $H_a = 0.5 \mu\text{m}$

The variation of oil film thickness in both axial and circumferential directions of smooth and rough surfaces is presented in Figure 14. This figure clearly shows the effect of the ridge's height on the oil film thickness. The minimum oil film thickness for smooth and rough bearings with ridges heights of 0, 0.1, 0.3 and 0.5 μm are 58.13, 57.80, 36.98 and 13.34 μm , respectively. The bearing with ridges of small height ($H_a = 0.1 \mu\text{m}$) behaves like a bearing with smooth surfaces since a percentage reduction in oil film thickness of 0.3 % is not exceeded, while it becomes 36.2 and 77 % for the bearings with rough surfaces that have higher ridges heights ($H_a = 0.3$ and 0.5 μm ,

respectively) in comparison with the bearing of smooth surfaces.

The variation in oil film pressure profiles in both axial and circumferential directions for smooth and rough bearings with different ridges heights is presented in Figure 15. The effect of surface irregularities is clearly shown for rough bearing with a higher roughness value.

6. Conclusions

In this study, the effect of surface roughness on the performance of three-lobe journal bearing considering cavitation and compressibility effects has been extensively numerically studied. The mathematical model was validated by comparing some of the obtained results with those published in the available literature. The following conclusions can be drawn:

- The oil film pressure and hence the load-carrying capacity of three-lobe journal bearing with microridges is significantly affected by the ridges high. A considerable enhancement was noticed in pressure and load-carrying capacity. However, considering the cavitation effect gives lower values of pressure.
- The coefficient of friction decreases by 15 % for the three-lobe journal bearing with higher ridges height when it works at lower eccentricity ratios.
- The end of the active zone of the three-lobe journal bearing increases for the bearing with higher values of ridges heights.
- Lubricant compressibility has little effect on the generated pressure of the rough three-lobe journal bearings.

Future work should be oriented to the study of the effect of different lubricants on the static and dynamic behaviour of the three-lobe journal bearing considering the effects of surface roughness, thermal effect and lubricant compressibility using the CFD technique.

Nomenclature

c	radial clearance, m
C_f	coefficient of friction
D	journal diameter, m
e	eccentricity, m
F_r	friction force, N
g	switch function
h	lubricant film thickness, m
\bar{h}	dimensionless lubricant film thickness

L	bearing length, m
N	rotational speed, rpm
P	hydrodynamic oil film pressure, Pa
\bar{P}	dimensionless hydrodynamic pressure
P_a	atmospheric pressure, Pa
P_{cav}	cavitation zone pressure, Pa
R	journal radius, m
U	tangential velocity, m/s
W	load-carrying capacity
\bar{W}_r	dimensionless radial load component
\bar{W}_t	dimensionless tangential load component
x, y, z	Cartesian coordinate system, m
\bar{z}	dimensionless axial coordinate
θ	lubricant bulk modulus, Pa
$\bar{\theta}$	dimensionless bulk modulus
Δ^*	dimensionless film thickness variation
ε	eccentricity ratio
ε_w	wave amplitude, μm
θ	circumferential coordinate, $^\circ$
μ	lubricant viscosity, Pas
μ_o	inlet lubricant viscosity, Pas
ρ	lubricant density, kg/m^3
ϕ	attitude angle, $^\circ$
φ	density ratio variable (fractional film content)

References

- [1] L. Roy, S.K. Kakoty, Groove location for optimum performance of three- and four-lobe bearings using genetic algorithm, Proceedings of the Institution of Mechanical Engineers, Part J: Journal of Engineering Tribology, Vol. 229, No. 1, 2015, pp. 47-63, DOI: [10.1177/1350650114541253](https://doi.org/10.1177/1350650114541253)
- [2] K. Qian, W.-G. Guo, Lubrication simulation and solution of oil film force and the equilibrium position of three-lobe journal bearing, in Proceedings of the International Conference on Material Science and Application (ICMMSA 2015), 13-14.06.2015, Suzhou, China, pp. 240-245, DOI: [10.2991/icmsa-15.2015.45](https://doi.org/10.2991/icmsa-15.2015.45)
- [3] N. Biswas, P. Chakraborti, A. Saha, S. Biswas, Performance & stability analysis of a three lobe journal bearing with varying parameters: Experiments and analysis, AIP Conference Proceedings, Vol. 1754, No. 1, 2016, Paper 030002, DOI: [10.1063/1.4958346](https://doi.org/10.1063/1.4958346)
- [4] I. Etsion, Modeling of surface texturing in hydrodynamic lubrication, Friction, Vol. 1, No. 3, 2013, pp. 195-209, DOI: [10.1007/s40544-013-0018-y](https://doi.org/10.1007/s40544-013-0018-y)
- [5] G. Bayada, S. Martin, C. Vázquez, Micro-roughness effects in (elasto)hydrodynamic lubrication including a mass-flow preserving cavitation model, Tribology International, Vol. 39, No. 12, 2006, pp. 1707-1718, DOI: [10.1016/j.triboint.2006.03.003](https://doi.org/10.1016/j.triboint.2006.03.003)
- [6] A. de Kraker, R.A.J. van Ostayen, D.J. Rixen, Development of a texture averaged Reynolds equation, Tribology International, Vol. 43, No. 11, 2010, pp. 2100-2109, DOI: [10.1016/j.triboint.2010.06.001](https://doi.org/10.1016/j.triboint.2010.06.001)
- [7] D.Y. Dhande, D.W. Pande, G.H. Lanjewar, Numerical analysis of three lobe hydrodynamic journal bearing using CFD-FSI technique based on response surface evaluation, Journal of the Brazilian Society of Mechanical Sciences and Engineering, Vol. 40, No. 8, 2018, Paper 393, DOI: [10.1007/s40430-018-1311-5](https://doi.org/10.1007/s40430-018-1311-5)
- [8] F.M. Meng, L. Zhang, Y. Liu, T.T. Li, Effect of compound dimple on tribological performances of journal bearing, Tribology International, Vol. 91, 2015, pp. 99-110, DOI: [10.1016/j.triboint.2015.06.030](https://doi.org/10.1016/j.triboint.2015.06.030)
- [9] R. Rahmani, I. Mirzaee, A. Shirvani, H. Shirvani, An analytical approach for analysis and optimisation of slider bearings with infinite width parallel textures, Tribology International, Vol. 43, No. 8, 2010, pp. 1551-1565, DOI: [10.1016/j.triboint.2010.02.016](https://doi.org/10.1016/j.triboint.2010.02.016)
- [10] R. Rahmani, H. Rahnejat, Enhanced performance of optimised partially textured load bearing surfaces, Tribology International, Vol. 117, 2018, pp. 272-282, DOI: [10.1016/j.triboint.2017.09.011](https://doi.org/10.1016/j.triboint.2017.09.011)
- [11] G. Caramia, G. Carbone, P. De Palma, Hydrodynamic lubrication of micro-textured surfaces: Two dimensional CFD-analysis, Tribology International, Vol. 88, 2015, pp. 162-169, DOI: [10.1016/j.triboint.2015.03.019](https://doi.org/10.1016/j.triboint.2015.03.019)
- [12] P. Lu, R.J.K. Wood, M.G. Gee, L. Wang, W. Pfleging, The use of anisotropic texturing for control of directional friction, Tribology International, Vol. 113, 2017, pp. 169-181, DOI: [10.1016/j.triboint.2017.02.005](https://doi.org/10.1016/j.triboint.2017.02.005)
- [13] M.-P. Noutary, N. Biboulet, A.A. Lubrecht, Dimple influence on load carrying capacity of parallel surfaces, Tribology International, Vol. 149, 2020, Paper 105452, DOI: [10.1016/j.triboint.2018.10.033](https://doi.org/10.1016/j.triboint.2018.10.033)
- [14] S. Cupillard, S. Glavatskih, M.J. Cervantes, 3D thermohydrodynamic analysis of a textured slider, Tribology International, Vol. 42, No. 10, 2009, pp. 1487-1495, DOI: [10.1016/j.triboint.2009.05.021](https://doi.org/10.1016/j.triboint.2009.05.021)
- [15] C. Ma, H. Zhu, An optimum design model for textured surface with elliptical-shape dimples under hydrodynamic lubrication, Tribology International, Vol. 44, No. 9, 2011, pp. 987-995, DOI: [10.1016/j.triboint.2011.04.005](https://doi.org/10.1016/j.triboint.2011.04.005)
- [16] A. Codrignani, B. Frohnepfel, F. Magagnato, P. Schreiber, J. Schneider, P. Gumbsch, Numerical and experimental investigation of texture shape and position in the macroscopic contact,

- Tribology International, Vol. 122, 2018, pp. 46-57, DOI: [10.1016/j.triboint.2018.02.001](https://doi.org/10.1016/j.triboint.2018.02.001)
- [17] K. PhaniRaja Kumar, S. Bhaskar, M. Manzoor Hussain, Analysis of multi lobe journal bearings with surface roughness using finite difference method, IOP Conference Series: Materials Science and Engineering, Vol. 346, 2018, Paper 012071, DOI: [10.1088/1757-899X/346/1/012071](https://doi.org/10.1088/1757-899X/346/1/012071)
- [18] T.V.V.L.N. Rao, A.M.A. Rani, N.M. Mohamed, H.H. Ya, M. Awang, F.M. Hashim, Static and stability analysis of partial slip texture multi-lobe journal bearings, Proceedings of the Institution of Mechanical Engineers, Part J: Journal of Engineering Tribology, Vol. 234, No. 4, 2020, pp. 567-587, DOI: [10.1177/1350650119882834](https://doi.org/10.1177/1350650119882834)
- [19] P.G. Grützmacher, A. Rosenkranz, A. Szurdak, F. König, G. Jacobs, G. Hirt, F. Mücklich, From lab to application – Improved frictional performance of journal bearings induced by single- and multi-scale surface patterns, Tribology International, Vol. 127, 2018, pp. 500-508, DOI: [10.1016/j.triboint.2018.06.036](https://doi.org/10.1016/j.triboint.2018.06.036)
- [20] F. König, A. Rosenkranz, P.G. Grützmacher, F. Mücklich, G. Jacobs, Effect of single- and multi-scale surface patterns on the frictional performance of journal bearings – A numerical study, Tribology International, Vol. 143, 2020, Paper 106041, DOI: [10.1016/j.triboint.2019.106041](https://doi.org/10.1016/j.triboint.2019.106041)
- [21] A.Kh. El-Said, B.M. El-Souhily, W.A. Crosby, H.A. El-Gamal, The performance and stability of three-lobe journal bearing textured with micro protrusions, Alexandria Engineering Journal, Vol. 56, No. 4, 2017, pp. 423-432, DOI: [10.1016/j.aej.2017.08.003](https://doi.org/10.1016/j.aej.2017.08.003)
- [22] H.-L. Chiang, C.-H. Hsu, J.-R. Lin, Lubrication performance of finite journal bearings considering effects of couple stresses and surface roughness, Tribology International, Vol. 37, No. 4, 2004, pp. 297-307, DOI: [10.1016/j.triboint.2003.10.005](https://doi.org/10.1016/j.triboint.2003.10.005)
- [23] M. Nabhani, M. El Khlifi, O.S.T. Gbehe, B. Bou-Saïd, Coupled couple stress and surface roughness effects on elasto-hydrodynamic contact, Lubrication Science, Vol. 26, No. 4, 2014, pp. 251-271, DOI: [10.1002/ls.1246](https://doi.org/10.1002/ls.1246)
- [24] M. Rom, S. Müller, An effective Navier-Stokes model for the simulation of textured surface lubrication, Tribology International, Vol. 124, 2018, pp. 247-258, DOI: [10.1016/j.triboint.2018.04.011](https://doi.org/10.1016/j.triboint.2018.04.011)
- [25] S. Zhu, J. Sun, B. Li, G. Zhu, Thermal turbulent lubrication analysis of rough surface journal bearing with journal misalignment, Tribology International, Vol. 144, 2020, Paper 106109, DOI: [10.1016/j.triboint.2019.106109](https://doi.org/10.1016/j.triboint.2019.106109)
- [26] N. Tala-Ighil, M. Fillon, A numerical investigation of both thermal and texturing surface effects on the journal bearings static characteristics, Tribology International, Vol. 90, 2015, pp. 228-239, DOI: [10.1016/j.triboint.2015.02.032](https://doi.org/10.1016/j.triboint.2015.02.032)
- [27] F. Sahlin, Hydrodynamic Lubrication of Rough Surfaces, MSc thesis, Luleå University of Technology, Luleå, 2005.
- [28] J.Y. Jang, M.M. Khonsari, On the wear of dynamically-loaded engine bearings with provision for misalignment and surface roughness, Tribology International, Vol. 141, 2020, Paper 105919, DOI: [10.1016/j.triboint.2019.105919](https://doi.org/10.1016/j.triboint.2019.105919)
- [29] C. Gu, X. Meng, Y. Xie, D. Zhang, Mixed lubrication problems in the presence of textures: An efficient solution to the cavitation problem with consideration of roughness effects, Tribology International, Vol. 103, 2016, pp. 516-528, DOI: [10.1016/j.triboint.2016.08.005](https://doi.org/10.1016/j.triboint.2016.08.005)
- [30] A. Venci, L. Ivanović, B. Stojanović, E. Zadorozhnaya, S. Miladinović, P. Svoboda, Surface texturing for tribological applications: A review, Proceedings on Engineering Sciences, Vol. 1, No. 1, 2019, pp. 227-239, DOI: [10.24874/PES01.01.029](https://doi.org/10.24874/PES01.01.029)
- [31] N. Miloradovic, B. Stojanovic, Tribological behaviour of ZA27/10SiC/1Gr hybrid composite, Journal of the Balkan Tribological Association, Vol. 19, No. 1, 2013, pp. 97-105.
- [32] N. Miloradović, R. Vujanac, B. Stojanović, A. Pavlović, Dry sliding wear behaviour of ZA27/SiC/Gr hybrid composites with Taguchi optimization, Composite Structures, Vol. 264, 2021, Paper 113658, DOI: [10.1016/j.compstruct.2021.113658](https://doi.org/10.1016/j.compstruct.2021.113658)
- [33] B. Manser, I. Belaidi, A. Hamrani, S. Khelladi, F. Bakir, Performance of hydrodynamic journal bearing under the combined influence of textured surface and journal misalignment: A numerical survey, Comptes Rendus Mécanique, Vol. 347, No. 2, 2019, pp. 141-165, DOI: [10.1016/j.crme.2018.11.002](https://doi.org/10.1016/j.crme.2018.11.002)
- [34] M.A. Mahdi, B.A. Abass, Effect of lubricant compressibility and variable viscosity on the performance of three-lobe journal bearing, Archive of Mechanical Engineering, Vol. 69, No. 2, 2022, pp. 203-219, DOI: [10.24425/ame.2022.140412](https://doi.org/10.24425/ame.2022.140412)
- [35] S. Cupillard, Thermohydrodynamics of Sliding Contacts with Textured Surfaces, PhD thesis, Luleå University of Technology, Luleå, 2009.
- [36] E.G. Elrod, M.L. Adams, A computer program for cavitation and starvation problems, in D. Dowson, M. Godet, C.M. Taylor (Eds.), Cavitation and Related Phenomena in Lubrication, Mechanical Engineering Publications, New York, 1975, pp. 37-41.